

# Intention Detection of Gait Adaptation in Natural Settings

Fani Deligianni, Ines Domingos, Guang-Zhong Yang, *Fellow, IEEE*

**Abstract**— Gait adaptation is an important part of gait analysis and its neuronal origin and dynamics has been studied extensively. In neurorehabilitation, it is important as it perturbs neuronal dynamics and allows patients to restore some of their motor function. Exoskeletons and robotics of the lower limbs are increasingly used to facilitate rehabilitation as well as supporting daily function. Their efficiency and safety depends on how well can sense the human intention to move and adapt the gait accordingly. This paper presents a gait adaptation scheme in natural settings. It allows monitoring of subjects in more realistic environment without the requirement of specialized equipment such as treadmill and foot pressure sensors. We extract gait characteristics based on a single RGB camera whereas wireless EEG signals are monitored simultaneously. We demonstrate that the method can not only successfully detect adaptation steps but also detect efficiently whether the subject adjust their pace to higher or lower speed.

## I. INTRODUCTION

In an aging population, gait assistive devices can support independent living of elderly people and help patient with neurological conditions. Several mechanisms have been suggested for patient-cooperative control of rehabilitation robots. For example, ankle rehabilitation devices normally depend on a predefined trajectory with limited ability to be adapted in real-time [1]. Simulation and validation of those devices is based on repetitive motion without significant gait adaptation differences.

Gait adaptation is essential in walking as it reflects the ability to change speed and direction to avoid obstacles and keep balance. Deficiencies in gait adaptation is an important index of several conditions, such as aging and neurological diseases like stroke and Parkinson's disease [2] [3] [4]. Furthermore, poor adaptability of exoskeletons and assistive devices limits their use and effectiveness in neuro-rehabilitation [5]. Therefore, identifying reliably the intention of the patient to adapt their gait would help future power exoskeletons to integrate seamlessly to rehabilitation practice.

In fact, robot-assisted training is an emerging technique for gait rehabilitation because it allows safe practicing as it can compensate the lack of motor control and muscle strength [6]. Robotic gait technology has shown to have positive effects on clinical outcomes of patients with stroke, spinal cord injury and Parkinson disease [7] [8] [9].

Following a neurological injury, such as stroke or spinal cord injury, the key to gait recovery, is neuroplasticity, which is an activity-dependent change in brain structure and function. For example, repetitive motion patterns enhance neuronal

connections involved in the underlying motor task but they could also trigger suboptimal compensation mechanism [10] [11]. Therefore, the timing of initiating therapeutic exercises and movements as well as the content of the exercises are of paramount importance.

To this end, gait adaptation based on split-zone treadmill exercises and auditory rhythm has shown to improve gait symmetry in patients with stroke, cerebral palsy and Parkinson disease [12] [13] [14]. Acoustically paced treadmill walking is an effective way to modify stride frequency and improve gait coordination in people after stroke [15]. Gait coordination is improved while patients try to couple heel strikes and pacing tones. However, without robotic support many patients cannot perform these exercises to an adequate level.

Recently, steady state visual evoked potentials (SSVEPs) have been proposed to control a lower-limb exoskeleton [16] [17]. SSEVPs are elicited from the visual cortex as a response to the repetitive fast presentation of stimulus. SSVEP-based brain computer interface (BCI) frameworks perform relatively well and they are characterized by low response time. However, SSVEPs is an indirect way of interfacing brain signals with machine and they do not reflect real human intention and motor control. Therefore, their use in neurorehabilitation is limited and it could be easily replaced from other assistive technologies, such as eye-tracking and voice control.

On the other hand, intention detection of movement and gait adaptation is well accepted as the best way to successfully integrate a lower limb robotic system. However, this depends on decoding EEG signal mainly from motor, premotor and frontal cortex. These brain regions along with subcortical regions form a complex network to control human movements that is challenging to decipher. Gait adaptation and the underlying neural dynamics have been extensively studied [2] [4] [18] [19] [20]. However, most of these experiments require the use of a treadmill and very specialized equipment. Gait events are measured based on either pressure sensors/insoles [18] [19] [20], reflective markers [4] or foot switches [2].

Here we study gait adaptation based on a rhythmic tone that alternates between three modes of slow, normal and fast pace. The subjects follow the tone as they walk inside a room without any further restriction. The EEG signal is simultaneously recorded via wireless devices. Contrary to previous studies we do not use a treadmill or specialized equipment, which allows the investigation of gait adaptation

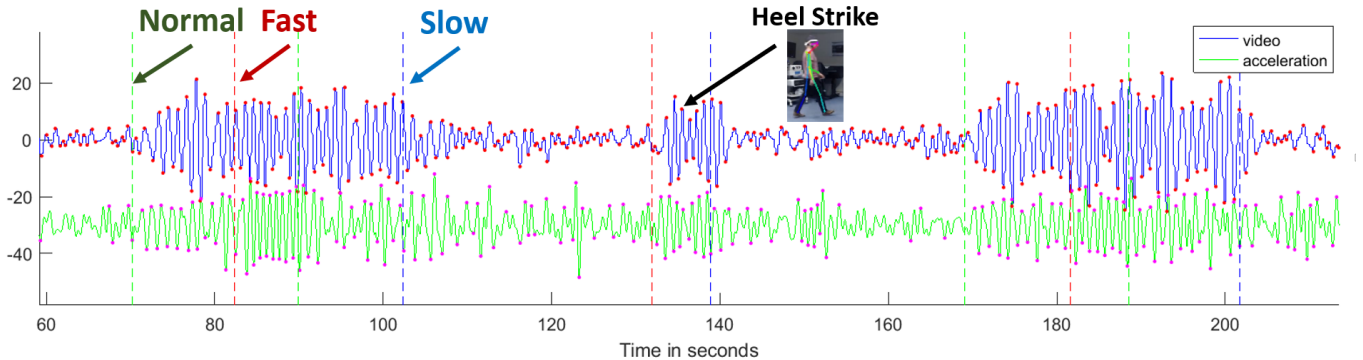


**Figure 1.** Gait feature extraction: The video-based gait signal and the acceleration-based gait signal are plotted in blue and green lines, respectively after SSA processing. The extrema points represent left and right heel strikes, respectively. Adaptation events are represented as vertical lines in green, red and blue colors that represent, normal, fast and slow speed, respectively.

in more natural settings. We capture gait characteristics such as heel strikes based on a single RGB camera. Subsequently, we use this information and behavioral analysis of the reaction time to extract gait adaptation steps versus non-gait adaptation steps.

We preprocess the EEG signal based on bandpass filtering and independent component analysis (ICA) to remove motion related artefacts and subsequently the signal is epoched based on right/left heel strikes. Finally, EEG gait adaptation characteristics are investigated based on three classification problems: i) right versus left gait cycle classification (two classes); ii) adaptation versus non adaptation steps (two classes) and iii) adaptation to higher pace versus adaptation steps towards lower pace versus non adaptation steps (three classes). To this end, we extract features based on regularized common spatial patterns (RCSP). CSP has been used successfully before for feature extraction in gait experiments [21]. Our results show that we can successfully discriminate adaptation versus non-adaptation with more than 90% testing accuracy, which corresponds to 0.06 10-fold cross-validated generalization loss. Based on sequential feature detection we figured out that five components are adequate to achieve good classification results.

## II. METHODS

### A. Experimental Setup and Procedures

EEG data was recorded from six healthy participants ( $27.5 \pm 7.58$  years). A 32-channels, g.tec Nautilus, EEG wireless acquisition system with active-electrodes (Ag/AgCl) was used. The system records EEG data at 250Hz along with acceleration data in three axes. The EEG cap was placed accordingly to the 10-20 system. Impedance was measured to ensure that each channel had less than  $30\Omega$  for all participants. Data were recorded with openvibe version 1.3 [22].

Participants were asked to walk according to a musical tone that it was programmed to switch between three modes, slow walking, normal walking and fast walking. The frequency at normal walking was 1.75Hz, whereas at slow walking speed was halved and in fast walking, speed was 1.5 times the normal. The duration of each mode was estimated to be around  $24 \pm 6$  right/left steps, which expresses a random variation of up to six steps. Each mode consisted of 20 trials,

which resulted in a total of 60 adaptations randomly permuted. The overall experiment lasts about 16 minutes. The stimulus was programmed and displayed with Psychtoolbox-3 [23] [24] [25]. Adaptation events were sent to the EEG acquisition server via TCP/IP communication.

A Logitech camera has been also used to record participants at 60 frames per second while they were walking. In order to synchronize the camera recording with the EEG acquisition, each captured frame raised an event that was sent to the EEG acquisition server via TCP/IP communication. Video capturing and events' transmission was also implemented with Psychtoolbox-3.

### B. Gait Features Extraction

We are interested in epoching the EEG signal into segments according to left/right heel strikes. Towards this aim, we obtain gait information based on the camera recordings and the acceleration data of the EEG system. To detect and track 2D coordinates of human joints based on a single RGB camera, we used OpenPose [26] [27] [28]. This is a state-of-the-art, real-time approach that uses deep neural networks to track the joints of multiple-persons stably.

Gait analysis based on a single RGB camera is challenging due to the perspective projection and limited 2D information [29]. To extract gait events of right and left heel strikes, we estimate the Euclidean distance between the left and right ankle coordinates in Y-camera axis, assuming that the camera is in a vertical position. Singular spectrum analysis (SSA) has been applied to denoise the signal and improve the detection of peaks that reflect foot contacts. SSA has been also used, successfully, to detect heel strikes based on acceleration data [30] [31].

SSA is based on time-series subsampling to construct a trajectory matrix, the so called Hankel matrix. If  $\mathbf{w}$  is a time-series, then the trajectory matrix takes the form:

$$W = \begin{pmatrix} w_0 & \cdots & w_{p-1} \\ \vdots & \ddots & \vdots \\ w_{l-1} & \cdots & w_{m-1} \end{pmatrix} \quad (1)$$

Where  $p = m - l + 1$ ,  $m$  is the length of  $\mathbf{w}$  and  $l$  is the embedding dimension. The signal is reconstructed from

averaging of a subset of the group elementary matrices of the decomposition of the covariance matrix:  $\mathbf{C}_W = \mathbf{W}\mathbf{W}^T$ .

Here we process acceleration data that comes with the gtec acquisition system to ensure that the EEG signal and the video timeline is fully synchronized. Acceleration data are processed with Principal Component Analysis (PCA) to derive the dominant signal variation, which is due to gait. Singular spectrum analysis (SSA) and peak detection was also utilized to detect heel strikes.

### C. Movement Artefact Removal

EEG-data acquisition is very sensitive to motion artefacts. To eliminate the influence of motion, we have filter the EEG signal based on a bandpass impulse response (FIR) filter of 3-45Hz. The filter is applied forward and then backward to ensure that phase delays are eliminated.

Subsequently, we use independent component analysis (ICA) based on the infomax algorithm to remove the influence of motion components [32]. ICA is a common approach of removing gait-related movement artefacts [33] [34]. It involves the extraction of maximally independent components. Motion components are normally identified manually based on their frequency profile and their spatial distribution. Subsequently, they are removed and the EEG signal is reconstructed without their influence.

### D. Feature Extraction based on Common Spatial Patterns

Here, we investigate gait adaptation by formulating a classification problem of whether a step is an adaptation step or not. We identify adaptation steps based on the reaction time (RT) between the change of the rhythmic tone and the step to match the average step of the session. Non-adaptation steps are drawn from the middle of the trial to match the number of the adaptation steps.

To extract classification features from the EEG data, we use the Common Spatial Patterns (CSP) algorithm, which extracts spatial filters that maximize the discriminability between two classes [35] [36]. CSP uses spatial filters  $s$  that maximize the following equations:

$$J(s) = \frac{s^T X_1^T X_1 s}{s^T X_2^T X_2 s} = \frac{s^T C_1 s}{s^T C_2 s} \quad (2)$$

$X_i$  denotes the matrix  $kn$  for class  $i$ , where  $k$  is the number of samples and  $n$  is the number of channels.  $C_i$  is the covariance matrix of the EEG signal from class  $i$ , assuming a zero mean.

This problem is transformed to a standard eigenvalue problem by noting that it is equivalent to maximizing the following function derived based on the Lagrange method [36]:

$$L(s) = s^T C_1 s - (s^T C_2 s - 1) \quad (3)$$

Since we are looking for the extreme points of the function the derivate of  $L$  with respect to  $s$  is zero and therefore:

$$C_2^{-1} C_1 s = s \quad (4)$$

#### 1) Regularised Common Spatial Patterns (RCSP)

Although, the CSP filters are an efficient way of extracting spatial filters that discriminate two classes, they are sensitive to noise and outliers. We have devised an automated way of

extracting right/left heel strikes that occasionally suffer from erroneous peak detection. To minimize the influence of these outliers in extracting features based on the CSP algorithm we use regularization.

We adopt the Ledoit and Wolf's method, which regularizes the covariance matrix by shrinking it to identity [37]. In other words, the goal is to find a linear combination of the identity matrix,  $\mathbf{I}$ , and the covariance matrix,  $\mathbf{C}_i$ , whose expected quadratic loss is minimum.

$$\mathbf{C}_i^* = (1 - \alpha)\mathbf{C}_i + \mathbf{I} \quad (5)$$

This method has been shown to be particularly effective in problems where the number of samples is less than the number of dimensions [38]. One of its major advantage is that the shrinkage parameter is estimated automatically based on the intrinsic properties of the signal.

#### 2) From two-class to multi-class formulation

We are interested in not only identifying the intention to adapt but also determining whether the adaptation is from a slower to faster pace or vice-versa. Therefore, we device a three-classes classification problem that includes adaptation to higher speed, adaptation to lower speed and non-adaptation. CSP and RCSP are intrinsically two-class methods. To overcome this problem, we construct three pairs of filters between each combination of the three classes.

## III. RESULTS

In this study, the investigation of gait and gait adaptation is based on the following EEG classification experiments:

- Right vs left gait cycle classification (two classes).
- Adaptation vs non adaptation steps (two classes).
- Adaptation to higher speed vs. adaptation steps towards lower speed vs. non adaptation steps (three classes).

TABLE I. BEHAVIORAL ANALYSIS OF ADAPTATION

Adaptation Type	Step statistics		
	Step duration (secs)	Adaptation time (secs)	Number of Adaptation steps
Slow	0.57±0.039	1.12±0.4	1.95±0.51
Normal	0.56±0.001	1.91±0.26	3.36±0.4
Fast	0.46±0.031	1.66±0.56	3.63±1.16

Table I summarises the behavioral analysis that includes the estimation of step time for each adaptation type: slow, normal and fast. It also includes the time and number of steps required to adapt from one condition to another. This is also called reaction time (RT) and it is estimated as the time between the change of the rhythmic tone and the time when the step matches the average step of the session within the standard deviation limit. We report a conservative RT, since we do not include the sessions where the end of adaption is not detected.

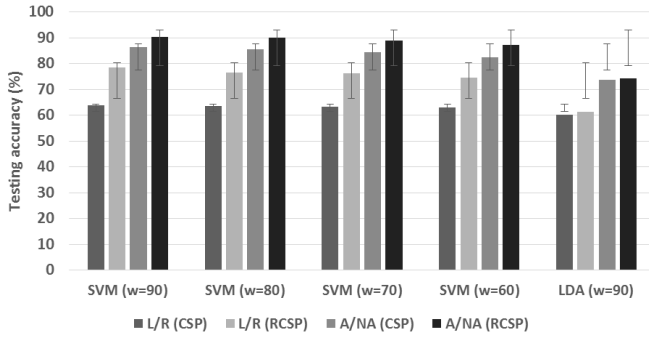


Figure 2. Testing accuracy of the classifications results of a) Left versus Right (L/R) steps and b) Adaptation versus non-adaptation (A/NA) steps. We compare results based on CSP and RCSP feature extraction. The results are shown across different sizes of sliding window (w).

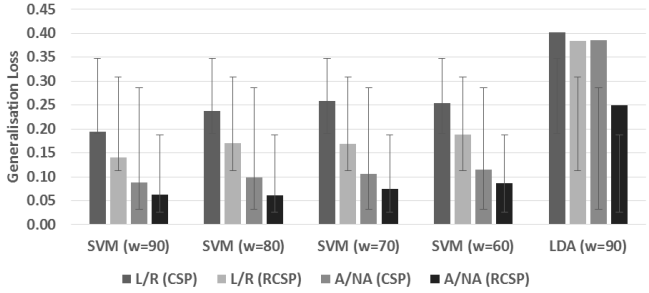


Figure 3. 10-fold cross-validation generalization loss of the classifications results of a) Left versus Right (L/R) steps and b) Adaptation versus non-adaptation (A/NA) steps. We compare results based on CSP and RCSP feature extraction. The results are shown across different sizes of sliding window (w).

The classification results for the right versus left gait cycles and for the adaptation versus non-adaptation steps are summarized in Figure 2 and Figure 3. Figure 2 demonstrates the testing accuracy of the classifications results of a) left versus right (L/R) steps and b) adaptation versus non-adaptation (A/NA) steps. We compare results based on CSP and RCSP feature extraction. The results are shown across different sizes of sliding window (w) with a range from 90 samples to 60 samples. Note that 90 samples correspond to 0.36 seconds, whereas the event duration is taken to be 0.4 seconds. In practice the step size may vary as it is shown in Table I. For the adaptation versus non-adaptation training/testing set we assumed that the first three steps after each change of rhythmic tone are adaptation steps and subsequently we chose three steps at the middle of each adaptation trial as the non-adaptation steps. For classification we used support vector machines (SVM) based on radial basis function but we also show the results based on linear discriminant analysis (LDA).

Figure 3 demonstrates the 10-fold cross-validation generalization loss of the classifications results of a) left versus right (L/R) steps and b) adaptation versus non-adaptation (A/NA) steps. We compare results based on CSP and RCSP feature extraction. The results are shown across different sizes of sliding window (w), similarly to Figure 2.

Table II demonstrates the average confusion matrix (percentage) across subjects for the three-class classification problem. Feature extraction was based on three RCSP filters for each combination of classes. Classification was performed based on SVM with a linear kernel to avoid overfitting. Results

are shown for a sliding window of 90 samples, which was shown to be most effective. The diagonal elements of the matrix represent the sensitivity results for each class. Note that the summation of the vertical columns results in 100%.

TABLE II. CONFUSION MATRIX (%) FOR THREE CLASS CLASSIFICATION

Predicted Class	Adaptation Type	True Class		
		Slow to faster	Faster to slower	Non-Adaptation
Slow to faster		84.79±4.66	5.08±3.32	8.69±2.49
Fast to slower		6.34±3.45	86.73±3.36	8.08±3.92
Non-adaptation		8.86±2.85	8.17±2.32	83.22±5.03

Figure 4 and Figure 5 demonstrate the analysis of the most significant RCSP components and their spatial distribution, respectively. Figure 4 shows the average across subjects, 10-fold cross-validation, generalisation loss as we pick more RCSP components from the most significant to less significant eigen values. We note that for both type of two-class classification the error drops significantly for the first five components but it remains the same or even increases when more components are incorporated.

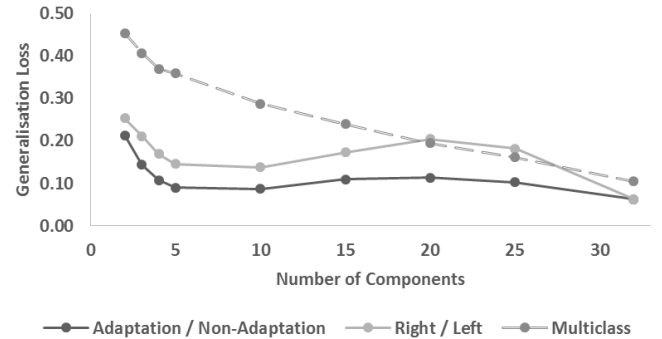


Figure 4. 10-fold cross-validation generalisation loss across the most significant RCSP components for a sliding window of 90 samples.

Figure 5 shows the spatial distribution of the five more significant RCSP components for one of the subjects. The top row shows the RCSP filters associated with adaptation/non-adaptation classification, whereas the middle row shows the RCSP filters associated with right/left classification. The bottom row shows the spatial distribution of the filters associated with adaptation towards higher pace versus adaptation towards lower pace.

## DISCUSSION

Gait adaptation plays a significant role in the ability of humans to walk and maintain their balance. In elderly and people with neurological problems, it is an index of their health progression. Therefore, exoskeletons and assistive robotic devices should be able to sense and quickly adjust to gait changes. This requires decoding neural signals accurately while people walk in their natural environments. Most of the adaptation studies today are based on specialized equipment

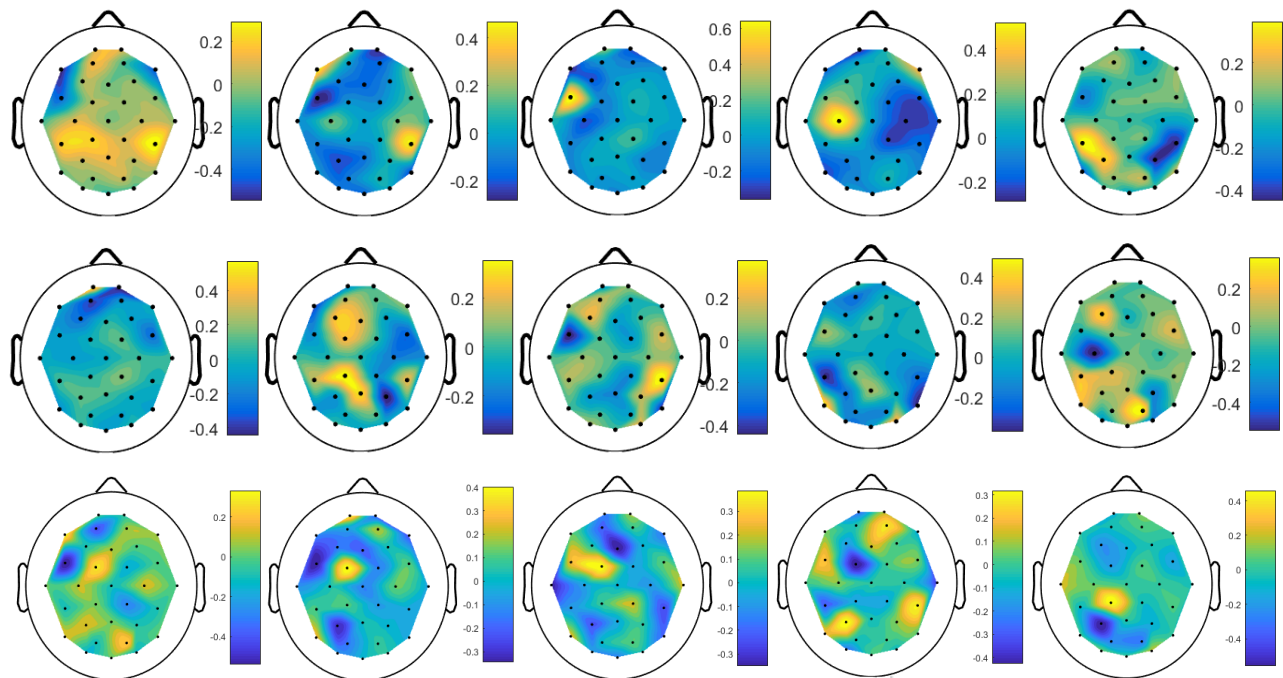


Figure 5. RCSP filters for the five most significant components of one of the subjects. a) Top row shows the RCSP filters associated with adaptation/non-adaptation classification, b) Middle row shows the RCSP filters associated with right/left classification, c) Bottom row shows the RCSP filters associated with the adaptation to higher versus adaptation to lower speed.

such as split-zone treadmill, whereas they monitor gait with pressure insoles or reflective markers/multi-camera systems. We have developed a framework to study gait adaptation in natural settings. The subjects walk in a room following the pace of a tone that changes between three modes of slow, normal and fast pace, randomly. We record EEG signal wirelessly whereas gait characteristics are extracted based on a single RGB camera.

The EEG signal is preprocessed based on a bandpass filter of 3-45 Hz, followed by ICA to identify and remove motion-related artefacts. We use the extracted gait characteristics to epoch the EEG signal and to formulate three classification problems of intention detection in gait adaptation: i) right versus left step, ii) adaptation steps versus non-adaptation steps and iii) adaptation to higher pace versus adaptation to lower pace versus non-adaptation. Subsequently, we use RCSP to extract EEG features that maximize the discriminability between two classes.

RCSP is a regularized version of CSP algorithm that allows for automatic regularization of the covariance matrices for each class. The extent of regularization depends on the intrinsic properties of the data. Here we note a significant improvement of our results based on the RCSP filters for all types of classification.

CSP/RCSP is intrinsically a two-class feature extraction method. To extend it to three classes we extract features from three pairs of classes: i) adaptation to higher pace vs non-adaptation, ii) adaptation to lower pace vs non-adaptation and iii) adaptation to lower pace versus adaptation to higher pace.

Finally, we investigate the influence of the number of

components to the classification accuracy and their spatial distribution. We note that for the two-class experiments five out of 32 components are enough to achieve high accuracy. Furthermore, the spatial distribution of the RCSP components seems to be of physiological origin.

#### ACKNOWLEDGMENT

We would like to acknowledge EPSRC (EP/R026092/1) funding and also to thank Jian-Qing Zheng, Jahanshah Fathi, Miao Sun and Dan-Dan Zhang.

#### REFERENCES

- [1] M. M. Zhang, S. Q. Xie, X. L. Li, G. L. Zhu, W. Meng, X. L. Huang, *et al.*, "Adaptive Patient-Cooperative Control of a Compliant Ankle Rehabilitation Robot (CARR) With Enhanced Training Safety," *Ieee Transactions on Industrial Electronics*, vol. 65, pp. 1398-1407, Feb 2018.
- [2] J. Wagner, S. Makeig, M. Gola, C. Neuper, and G. Muller-Putz, "Distinct beta Band Oscillatory Networks Subservicing Motor and Cognitive Control during Gait Adaptation," *Journal of Neuroscience*, vol. 36, pp. 2212-2226, Feb 17 2016.
- [3] J. T. Gwin, K. Gramann, S. Makeig, and D. P. Ferris, "Electrocortical activity is coupled to gait cycle phase during treadmill walking," *Neuroimage*, vol. 54, pp. 1289-1296, Jan 15 2011.
- [4] D. Martelli, V. Vashista, S. Micera, and S. K. Agrawal, "Direction-Dependent Adaptation of Dynamic Gait Stability Following Waist-Pull Perturbations," *Ieee Transactions on Neural Systems and Rehabilitation Engineering*, vol. 24, pp. 1304-1313, Dec 2016.
- [5] D. A. Jacobs, J. R. Koller, K. M. Steele, and D. P. Ferris, "Motor modules during adaptation to walking in a powered ankle

- exoskeleton," *Journal of Neuroengineering and Rehabilitation*, vol. 15, Jan 3 2018.
- [6] S. E. Fasoli, H. I. Krebs, J. Stein, W. R. Frontera, R. Hughes, and N. Hogan, "Robotic therapy for chronic motor impairments after stroke: Follow-up results," *Archives of Physical Medicine and Rehabilitation*, vol. 85, pp. 1106-1111, Jul 2004.
- [7] B. Husemann, F. Muller, C. Krewer, S. Heller, and E. Koenig, "Effects of locomotion training with assistance of a robot-driven gait orthosis in hemiparetic patients after stroke - A randomized controlled pilot study," *Stroke*, vol. 38, pp. 349-354, Feb 2007.
- [8] A. Picelli, C. Melotti, F. Origano, A. Waldner, A. Fiaschi, V. Santilli, *et al.*, "Robot-Assisted Gait Training in Patients With Parkinson Disease: A Randomized Controlled Trial," *Neurorehabilitation and Neural Repair*, vol. 26, pp. 353-361, May 2012.
- [9] S. C. Hayes, C. R. James Wilcox, H. S. Forbes White, and N. Vanicek, "The effects of robot assisted gait training on temporal-spatial characteristics of people with spinal cord injuries: A systematic review," *J Spinal Cord Med*, pp. 1-15, Feb 5 2018.
- [10] T. A. Jones, "Motor compensation and its effects on neural reorganization after stroke," *Nature Reviews Neuroscience*, vol. 18, pp. 267-280, May 2017.
- [11] V. R. Edgerton, R. D. de Leon, N. Tillakaratne, M. R. Recktenwald, J. A. Hodgson, and R. R. Roy, "Use-dependent plasticity in spinal stepping and standing," *Adv Neurol*, vol. 72, pp. 233-47, 1997.
- [12] M. H. Thaut and M. Abiru, "Rhythmic Auditory Stimulation in Rehabilitation of Movement Disorders: A Review of Current Research," *Music Perception*, vol. 27, pp. 263-269, Apr 2010.
- [13] M. Roerdink, C. J. C. Lamoth, J. van Kordelaar, P. Elich, M. Konijnenbelt, G. Kwakkel, *et al.*, "Rhythm Perturbations in Acoustically Paced Treadmill Walking After Stroke," *Neurorehabilitation and Neural Repair*, vol. 23, pp. 668-678, Sep 2009.
- [14] T. E. Howe, B. Lovgreen, F. W. J. Cody, V. J. Ashton, and J. A. Oldham, "Auditory cues can modify the gait of persons with early-stage Parkinson's disease: a method for enhancing parkinsonian walking performance?," *Clinical Rehabilitation*, vol. 17, pp. 363-367, Jul 2003.
- [15] M. Roerdink, C. J. C. Lamoth, G. Kwakkel, P. C. W. van Wieringen, and P. J. Beek, "Gait coordination after stroke: Benefits of acoustically paced treadmill walking," *Physical Therapy*, vol. 87, pp. 1009-1022, Aug 2007.
- [16] N. S. Kwak, K. R. Muller, and S. W. Lee, "A lower limb exoskeleton control system based on steady state visual evoked potentials," *Journal of Neural Engineering*, vol. 12, Oct 2015.
- [17] N. S. Kwak, K. R. Muller, and S. W. Lee, "A convolutional neural network for steady state visual evoked potential classification under ambulatory environment," *Plos One*, vol. 12, Feb 22 2017.
- [18] S. M. Bruijn, J. H. Van Dieen, and A. Daffertshofer, "Beta activity in the premotor cortex is increased during stabilized as compared to normal walking," *Frontiers in Human Neuroscience*, vol. 9, Oct 27 2015.
- [19] L. Fernandez, N. Albein-Urios, M. Kirkovski, J. L. McGinley, A. T. Murphy, C. Hyde, *et al.*, "Cathodal Transcranial Direct Current Stimulation (tDCS) to the Right Cerebellar Hemisphere Affects Motor Adaptation During Gait," *Cerebellum*, vol. 16, pp. 168-177, Feb 2017.
- [20] J. C. Bradford, J. R. Lukos, and D. P. Ferris, "Electrocortical activity distinguishes between uphill and level walking in humans," *Journal of Neurophysiology*, vol. 115, pp. 958-966, Feb 1 2016.
- [21] C. Zhang, S. Bengio, M. Hardt, B. Recht, and O. Vinyals, "Understanding deep learning requires rethinking generalization," *arXiv preprint arXiv:1611.03530*, 2016.
- [22] Y. Renard, F. Lotte, G. Gibert, M. Congedo, E. Maby, V. Delannoy, *et al.*, "OpenViBE: An Open-Source Software Platform to Design, Test, and Use Brain-Computer Interfaces in Real and Virtual Environments," *Presence-Teleoperators and Virtual Environments*, vol. 19, pp. 35-53, Feb 2010.
- [23] D. H. Brainard, "The psychophysics toolbox," *Spatial Vision*, vol. 10, pp. 433-436, 1997.
- [24] D. G. Pelli, "The VideoToolbox software for visual psychophysics: Transforming numbers into movies," *Spatial Vision*, vol. 10, pp. 437-442, 1997.
- [25] M. Kleiner, D. Brainard, and D. Pelli, "What's new in Psychtoolbox-3?," *Perception*, vol. 36, pp. 14-14, 2007.
- [26] Z. Cao, T. Simon, S. E. Wei, and Y. Sheikh, "Realtime Multi-Person 2D Pose Estimation using Part Affinity Fields," *30th Ieee Conference on Computer Vision and Pattern Recognition (Cvpr 2017)*, pp. 1302-1310, 2017.
- [27] S. E. Wei, V. Ramakrishna, T. Kanade, and Y. Sheikh, "Convolutional Pose Machines," *2016 Ieee Conference on Computer Vision and Pattern Recognition (Cvpr)*, pp. 4724-4732, 2016.
- [28] T. Simon, H. Joo, I. Matthews, and Y. Sheikh, "Hand Keypoint Detection in Single Images using Multiview Bootstrapping," *30th Ieee Conference on Computer Vision and Pattern Recognition (Cvpr 2017)*, pp. 4645-4653, 2017.
- [29] X. D. Gu, F.; Lo, B.; Chen, W.; Yang, G., "Markerless Gait Analysis Based on a Single RGB Camera," presented at the International Conference on Wearable and Implantable Body Sensor Networks, Las Vegas, NV, USA, 2018.
- [30] D. Jarchi, C. Wong, R. M. Kwasnicki, B. Heller, G. A. Tew, and G. Z. Yang, "Gait Parameter Estimation From a Miniaturized Ear-Worn Sensor Using Singular Spectrum Analysis and Longest Common Subsequence," *Ieee Transactions on Biomedical Engineering*, vol. 61, pp. 1261-1273, Apr 2014.
- [31] F. Deligianni, C. Wong, B. Lo, and G. Z. Yang, "A fusion framework to estimate plantar ground force distributions and ankle dynamics," *Information Fusion*, vol. 41, pp. 255-263, May 2018.
- [32] S. Makeig, A. J. Bell, T. P. Jung, and T. J. Sejnowski, "Independent component analysis of electroencephalographic data," *Advances in Neural Information Processing Systems 8*, vol. 8, pp. 145-151, 1996.
- [33] K. L. Snyder, J. E. Kline, H. J. Huang, and D. P. Ferris, "Independent Component Analysis of Gait-Related Movement Artifact Recorded using EEG Electrodes during Treadmill Walking," *Frontiers in Human Neuroscience*, vol. 9, Dec 1 2015.
- [34] J. T. Gwin, K. Gramann, S. Makeig, and D. P. Ferris, "Removal of Movement Artifact From High-Density EEG Recorded During Walking and Running," *Journal of Neurophysiology*, vol. 103, pp. 3526-3534, Jun 2010.
- [35] F. Lotte and C. T. Guan, "Regularizing Common Spatial Patterns to Improve BCI Designs: Unified Theory and New Algorithms," *Ieee Transactions on Biomedical Engineering*, vol. 58, pp. 355-362, Feb 2011.
- [36] F. G. Lotte, C., "Spatially Regularized Common Spatial Patterns for EEG Classification," presented at the 20th International Conference on Pattern Recognition, 2010.
- [37] O. Ledoit and M. Wolf, "A well-conditioned estimator for large-dimensional covariance matrices," *Journal of Multivariate Analysis*, vol. 88, pp. 365-411, Feb 2004.
- [38] F. Deligianni, G. Varoquaux, B. Thirion, D. J. Sharp, C. Ledig, R. Leech, *et al.*, "A Framework for Inter-Subject Prediction of Functional Connectivity From Structural Networks," *Ieee Transactions on Medical Imaging*, vol. 32, pp. 2200-2214, Dec 2013.